Influence of Al_2O_3 nanoparticles on the isothermal cure of an epoxy resin

2009 J. Phys.: Condens. Matter 21 035118

(http://iopscience.iop.org/0953-8984/21/3/035118)

J. Phys.: Condens. Matter **21** (2009) 035118 (8pp) doi:10.1088/0953-8984/21/3/035118

Influence of Al_2O_3 nanoparticles on the isothermal cure of an epoxy resin

R Sanctuary, J Baller, B Zielinski, N Becker, J K Krüger, M Philipp, U Müller and M Ziehmer

University of Luxembourg, 162a avenue de la Faïencerie, L-1511, Luxembourg

E-mail: roland.sanctuary@uni.lu

Received 15 July 2008, in final form 24 October 2008
Published 15 December 2008
Online at stacks.iop.org/JPhysCM/21/035118

Abstract

The influence of Al_2O_3 nanoparticles on the curing of an epoxy thermoset based on diglycidyl ether of bisphenol A was investigated using temperature-modulated differential scanning calorimetry (TMDSC) and rheology. Diethylene triamine was used as a hardener. TMDSC not only allows for a systematic study of the kinetics of cure but simultaneously gives access to the evolution of the specific heat capacities of the thermosets. The technique thus provides insight into the glass transition behaviour of the nanocomposites and hence makes it possible to shed some light on the interaction between the nanoparticles and the polymer matrix. The Al_2O_3 fillers are shown to accelerate the growth of macromolecules upon isothermal curing. Several mechanisms which possibly could be responsible for the acceleration are described. As a result of the faster network growth chemical vitrification occurs at earlier times in the filled thermosets and the specific reaction heat decreases with increasing nanoparticle concentration. Rheologic measurements of the zero-shear viscosity confirm the faster growth of the macromolecules in the presence of the nanoparticles.

(Some figures in this article are in colour only in the electronic version)

1. Introduction

Epoxies are reactive network-forming polymer systems with outstanding behaviour as adhesives or coatings. During the last few years a lot of effort has been made to improve the mechanical, tribological and adhesive properties of these materials without abandoning features like low specific weight, good processability, transparency or high resistance to degradation. It has been shown [1–9] that the incorporation of appropriate nanoparticles into the epoxy yields nanocomposites with mechanical properties superior to the neat matrix. Thus, for instance, small amounts of alumina nanoparticles (1–2 vol%) dispersed in an epoxy matrix simultaneously improve its stiffness and impact strength whereas failure strain is increased [1]. Interfacial interactions emerging at the extended surfaces of the fillers are generally made responsible for the new or improved behaviour of the nanorefined polymer matrices. Using nanoparticles to functionalize the polymer matrix is generally impossible without influencing the processing of the nanocomposites. Ji *et al* [2] have investigated the influence of alumina particles on the reaction kinetics of an epoxy at temperatures higher than 373 K. They showed that the fillers have an accelerating effect on dynamic curing (curing upon heating) of the epoxy resin. Hydroxyl groups populating the surface of the fillers and interaction forces between the nanoparticles and the reactants leading to increased 'local' concentrations of resin and hardener molecules are made responsible for the higher reaction rates. The authors refer to the free volume hypothesis introduced by Paz-Abuin *et al* [10] and exploited by Altmann *et al* [11] to explain the reaction kinetics of epoxy–amine thermosets filled with micrometre-sized silica.

The present work mainly focuses on the influence of Al_2O_3 nanoparticles on the isothermal cure of epoxy resins. The aim consists in getting more insight into the manner Al_2O_3 nanoparticles participate in the epoxy network formation, have influence on gelation and modify the overall molecular mobility inside the reacting system. Some light will also be shed on the impact of the Al_2O_3 nanoparticles on the reaction kinetics of the chosen epoxy model system and its transition from a chemically controlled regime into a diffusion controlled regime. As experimental techniques temperature-modulated differential scanning calorimetry (TMDSC) and rheology are used. TMDSC [12, 13] is a well-suited tool

to study isothermal curing, because reaction-induced changes of specific heat capacity and heat flow intensity can be investigated simultaneously. The technique thus allows for monitoring the evolution of the reaction, determining specific reaction heats and studying the chemical glass transition induced by the decrease of molecular mobility as a result of the network formation. In the course of network formation chemical gelation occurs when the material changes from the initial viscous state to a rubbery state because covalent bonds connect across the whole volume of the curing system [14]. This critical liquid-to-rubber transition arises when the mass average molecular mass and consequently the zero-shear viscosity diverge to infinity [14]. In this work the zero-shear viscosity is obtained from steady shear tests performed at different stages of the network formation [15, 16].

2. Materials, sample preparation and experimental details

2.1. Materials and sample preparation

The model thermosetting epoxy system investigated in this work is DER331 (Dow Chemical), a resin based on diglycidyl ether of bisphenol A (DGEBA) and DETA (diethylene triamine from Fluka). The reaction mechanism is well known and described elsewhere [17, 18]. The fillers are AEROXIDE® Alu C aluminium oxide nanoparticles produced by EVONIK industries. The primary particles are not surface treated and have an average diameter of 13 nm. van der Waals forces and chemical bonds are responsible for the formation of agglomerates and aggregates of Al_2O_3 particles with sizes far beyond the nanoscale. A mother batch of DER331 refined with $x = 28.9\%$ of Al_2O_3 ($x = \frac{m_{Al_2O_3}}{m_{DER331}+m_{Al_2O_3}}$) is obtained by dispersing the fillers inside the oligomer matrix. Scanning electron microscopy (SEM) reveals that mechanical dispersing involving a dissolver and a bead mill finally yields a rather homogeneous distribution of Al_2O_3 aggregates inside the matrix (figure 1). Assuming that the orientation of the clusters is isotropic, the SEM picture allows for claiming that the average size of the nanoparticles is smaller than 100 nm. Besides of drying the nanoparticles at 70 °C before dispersing them into the oligomer matrix, no particular measures have been taken to avoid the adsorption of water on the filler's surfaces. We therefore cannot exclude that the Al_2O_3 surfaces are contaminated with water. The DER331–x% Al_2O_3 (x = 7.2, 11.6 and 15.8) resins used in this work are obtained by adequately diluting the DER331–28.9% Al_2O_3 mother batch with the pure resin DER 331.

The curing process is started by injecting the hardener into the DER331–x% Al_2O_3 resin. For all the samples a mixing ratio $m_{DETA}/m_{DER331} = 14$ g/100 g is respected. Resin and hardener mixed in this ratio are known to yield adhesives with a maximum bond strength to aluminium substrates [21]. Compared to the stoichiometric ratio (11 g/100 g), the preparation provides an excess of amine hardener.

After stirring the samples by hand for 5 min at $T_{stir} = (298 \pm 1)$ K, the reactive mixtures with masses $m = 14$–20 mg are either isothermally cured under a nitrogen atmosphere in a differential scanning calorimeter respectively a rheometer at $T_{cure} = 298$ K or quenched to liquid nitrogen temperature to perform dynamic cure experiments.

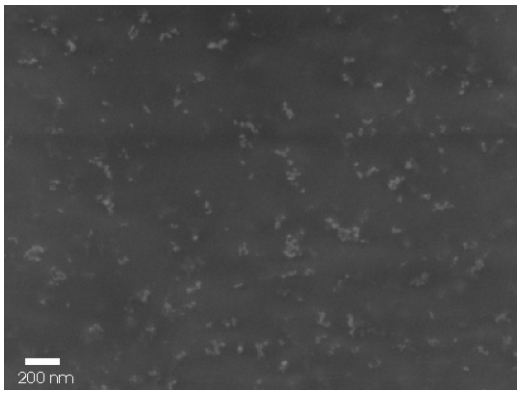

Figure 1. SEM picture of a DER331–4.8% Al_2O_3–DETA sample (secondary electron imaging modus). The surface of the sample has been kindly prepared by JEOL (Europe) BV by means of a cross-section polisher.

2.2. Calorimetric measurements

The TMDSC measurements are performed on a METTLER TOLEDO DSC 823e. The instrument is temperature- and heat flow-calibrated using water, indium, naphthalene and benzoic acid. In a TMDSC experiment the calorimeter furnace is controlled by the following temperature programme:

$$T(t) = T_0 + \beta t + T_a \sin \omega t. \tag{1}$$

In our isothermal curing experiments, $T_0 = 298$ K, $\beta = 0$, the temperature amplitude is $T_a = 0.5$ K and the angular frequency $\omega = \frac{2\pi}{t_p} = 0.052$ rad s^{-1}, with $t_p = 120$ s representing the modulation period.

In the frame of linear response theory the heat flow intensity HF into the sample can be written as [19]

$$\mathrm{HF} = \mathrm{HF_u} + \mathrm{HF_a} \cos(\omega t - \varphi). \tag{2}$$

This signal can be deconvoluted in order to get the underlying heat flow intensity HF_u, the amplitude HF_a of the modulated heat flow intensity and the phase angle φ between the measured heat flow and the temperature rate. HF_u is related to the conventional DSC curve. In case of an isothermal cure experiment HF_u is proportional to the calorimetric reaction rate. The modulus of the specific complex heat capacity (at constant pressure) c_p is determined from the respective amplitudes of the temperature T_a and the heat flow intensity HF_a:

$$|c_p| = \frac{K \mathrm{HF_a}}{m T_a \omega} \tag{3}$$

where m is the sample mass. The calibration factor K is obtained using an aluminium standard with well-known specific heat capacity.

The calculation of chemical conversion:

$$\alpha(t) = \frac{\int_0^t \mathrm{HF_u}(t')\,\mathrm{d}t'}{\Delta H_{total}} \tag{4}$$

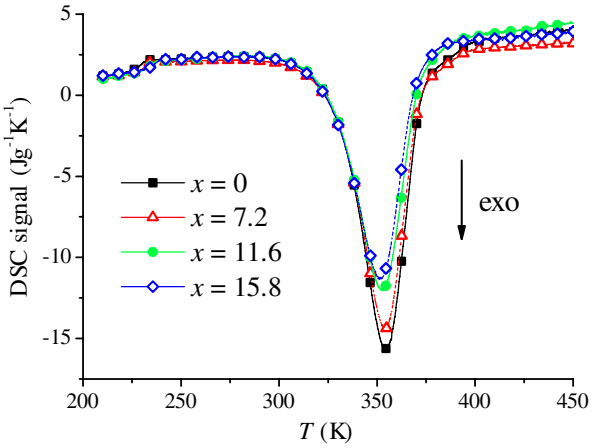

Figure 2. DSC signals obtained from dynamic scans of DER331–x% Al_2O_3–DETA nanocomposites after stirring at 298 K and subsequent quenching to liquid nitrogen temperature. The scanning range extends from 210 to 450 K; the heating rate is $\beta = +3$ K min^{-1}. While the lines correspond to measured data the symbols help to differentiate between the four investigated nanocomposites.

and reaction rate $\frac{d\alpha}{dt}$ requires a knowledge of ΔH_{total}, the total reaction heat per gram epoxy. ΔH_{total} is obtained from dynamic cure experiments using conventional DSC ($T_0 = 200$ K, $\beta = 3$ K min^{-1}, $T_a = 0$; see (1)). Dynamic cure is run on those samples which have been quenched to liquid nitrogen temperature. Quenching is necessary to stop the reaction of the samples during the time needed to settle the start temperature of the calorimeter. The scanning range extends from 200 to 450 K.

2.3. Rheologic measurements

A linear viscoelastic liquid can be characterized by a shear viscosity coefficient defined as

$$\eta = \frac{d\tau}{d\dot{\gamma}} \tag{5}$$

with τ representing the stress required to establish a shear rate $\dot{\gamma} = \frac{d\gamma}{dt}$. In order to determine the zero-shear viscosity:

$$\eta_0 = \left.\frac{d\tau}{d\dot{\gamma}}\right|_{\dot{\gamma}\to 0} \tag{6}$$

at given cure times t_{cure}, steady shear flow curves $\tau(\dot{\gamma})$ are recorded by means of a HAAKE MARS II rheometer [16]. The most common used plate–plate geometry comes into operation with a diameter of 20 mm and a gap of 1 mm. Each of the samples, prepared as described in section 2.2, is placed in the instrument at $T_{\text{cure}} = 298$ K. In order to avoid the heating-up of the samples by the importing of too large quantities of mechanical energy, the sweeping range of $\dot{\gamma}$ is continuously reduced as the reaction progresses. This method allows us to keep the curing temperature constant at $T_{\text{cure}} = (298.0 \pm 1.5)$ K. η_0 is obtained from the flow curves by extrapolating the lower Newtonian plateau to $\dot{\gamma} = 0$.

Table 1. Total specific reaction heat ΔH_{total} obtained from dynamic cure experiments as a function of Al_2O_3 nanoparticle mass concentration x. $\Delta H_{\text{total epoxy}}$ represents the total reaction heat per gram epoxy calculated from ΔH_{total} and ΔH_{epoxy} corresponds to the reaction heat per gram epoxy released upon isothermal curing at $T_{\text{cure}} = 298$ K. With an epoxy equivalent weight of 185 g mol^{-1} for DER331, a total reaction heat of 567 J g^{-1} (obtained for the neat epoxy) corresponds to 120 kJ per epoxy equivalent.

x	ΔH_{total} (J g^{-1})	$\Delta H_{\text{total epoxy}}$ (J g^{-1})	ΔH_{epoxy} (J g^{-1})
0	567 ± 11	567 ± 11	400
7.2	512 ± 10	546 ± 11	386
11.6	487 ± 10	543 ± 11	367
15.8	444 ± 9	517 ± 10	359

3. Results and discussion

Figure 2 shows for each of the initially uncured samples the DSC signal $\text{DSC}(T) = \beta^{-1} \cdot \text{HF}(T)$ as a function of temperature, $\text{HF}(T)$ representing the heat flow intensity at temperature T and β the heating rate. The steps at around 225 K correspond to the glass transitions of the reactive mixtures. It appears that the Al_2O_3 nanoparticles have an influence on the total reaction heat released by the samples. The start of the network formation is visualized by the onsets of the peaks corresponding to the exothermic epoxy–amine reactions. During the first stage of the reaction all of the DSC curves practically coincide. Obviously, at the beginning of the dynamic cure experiments, the generation of predominantly linear molecules is not significantly hindered by the nanoparticles. At intermediate stages of the cure process, however, the reaction heat significantly depends on the concentration of the alumina. At temperatures higher than 375 K the DSC curves for $x = 0$, respectively $x = 7.2$, exhibit reproducible anomalies which are indicative for further exothermal events. We assume that the additional heat is produced by reactions taking place in the diffusion-controlled regime and involving hydroxide groups generated when oxirane rings react with primary and secondary amine groups. As a matter of fact we know from the neat epoxy system that the reaction of hydroxide groups with oxirane rings is only possible at high temperatures or in the presence of catalysts [20]. In the samples with higher nanoparticle concentrations ($x = 11.6$ or 15.8), the absence of the reaction mechanism involving the hydroxide groups remains to be investigated. It could result from the hindrance of diffusion of the reactants by the fillers. For each of the samples the total reaction heat ΔH_{total} has been determined from the curves in figure 2 by drawing a straight line connecting the baseline before and after the reaction peak and integrating the peak area limited by the baseline. Table 1 shows average values of ΔH_{total} and $\Delta H_{\text{total epoxy}}$ calculated for several identically prepared samples with the same thermal history. These values do not include the reaction heat produced during the five minutes of mixing by hand. We have calculated that this contribution is negligible with respect to the measurement inaccuracies indicated in table 1. While ΔH_{total} corresponds to the specific reaction heat calculated using the total mass of the sample, $\Delta H_{\text{total epoxy}}$ indicates the specific reaction heat with

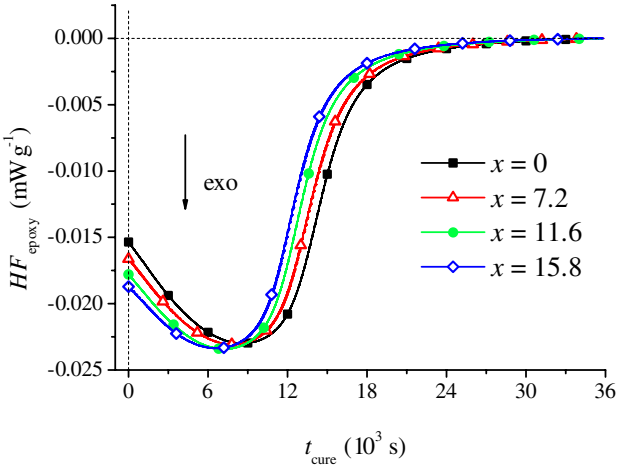

Figure 3. Isothermal cure of DER331–x% Al_2O_3–DETA nanocomposites at $T_{cure} = 298$ K: heat flow intensities per gram epoxy HF_{epoxy} as a function of curing time t_{cure}.

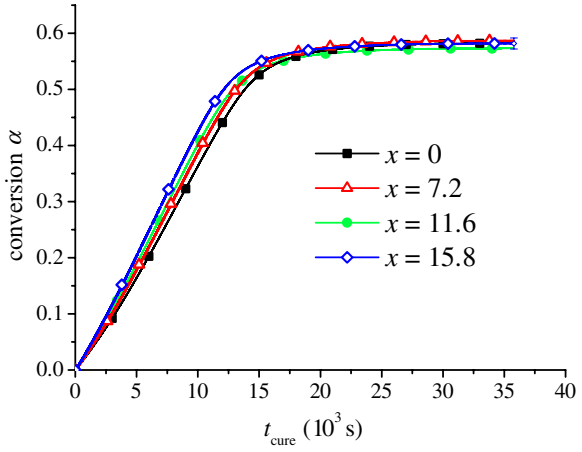

Figure 4. Isothermal cure of DER331–x% Al_2O_3–DETA nanocomposites at $T_{cure} = 298$ K: conversion α as a function of curing time t_{cure}. Conversions are calculated using the proper total reaction heat produced by each nanocomposite.

respect to the epoxy content. Obviously the total reaction heat per gram epoxy decreases by around 9% when the nanoparticle mass concentration increases from 0 to 15.8%.

Figure 3 shows for each of the investigated nanocomposites how the heat flow intensity per gram epoxy evolves during isothermal cure at $T_{cure} = 298$ K. Assuming in a first approximation that, after chemical vitrification, the reaction rates have dropped to zero at the end of ten hours of isothermal cure we have adjusted the curves in such a way that at $t_{cure} = 10$ h the heat flow intensities HF_{epoxy} reach the baseline. For practical reasons the calorimetric measurements can start only 5–7 min after mixing together the resin and the hardener.

As we want to estimate the total reaction heat produced in the course of the isothermal cure experiments we have extrapolated the measured heat flow curves to $t = 0$ by constructing tangents to the onsets of the graphs. Interestingly, at the beginning of the reaction, the reaction rate (proportional to $|HF_{epoxy}|$) is the higher the larger the filler content in the sample. This behaviour, which we believe to be related to a catalytic effect of the nanoparticles, is dominating until the respective $|HF_{epoxy}|$ curves reach their maximum values.

Astonishingly, in the dynamic cure experiments described above (figure 2), there is no indication for a catalytic impact of the nanoparticles. Apparently the continuously increasing thermal activation of the reaction is dominating with respect to such a catalytic action. From figure 3 it further becomes clear that the time corresponding to the maximum value of the reaction rate systematically decreases with increasing Al_2O_3 content. Obviously the slowing down of the reaction also occurs earlier the higher the nanoparticle concentration. The total reaction heats per gram epoxy ΔH_{epoxy} produced during 10 h of isothermal cure are listed in table 1. The values correspond to the areas limited by the baseline and the heat flow curves. Similarly to the total reaction heat per gram epoxy listed in table 1, ΔH_{epoxy} decreases when the nanoparticle concentration gets larger.

Chemical vitrification emerging when the glass transition temperature of the growing network exceeds the curing temperature $T_{cure} = 298$ K ($T_{cure} < T_{G\infty}$; $T_{G\infty}$: glass transition temperature of the fully cured network) hinders the reactions to progress. From this it follows that the chemical conversions are lower than unity ($\Delta H_{epoxy} < \Delta H_{epoxy\ total}$) after 10 h of isothermal cure. The conversions $\alpha(t_{cure})$ calculated from the data represented in figure 3 and table 1 are shown in figure 4.

At the beginning of cure the acceleration of the reaction by the nanoparticles is obvious. After 10 h of isothermal cross-linking each of the nanocomposites reaches a final conversion $\alpha_{final} = 0.58 \pm 0.01$ which in the margins of experimental accuracy corresponds to the chemical turnover of the neat epoxy. This result can better be understood by considering that the conversions have been calculated using the proper total reaction heats of the respective nanocomposites. It is evident that conversions computed by means of the total reaction heat of neat epoxy would be smaller than the turnovers represented in figure 4. Numerical derivation of the curves in figure 4 yields the reaction rates $\frac{d\alpha}{dt}$. In figure 5 we have represented $\frac{d\alpha}{dt}$ as a function of conversion α.

As long as the investigated systems evolve in the chemically controlled regime [21] where mobility restrictions are negligible, the reactions are modelled by semi-empirical Kamal equations taking into account autocatalytic nth-order kinetics [22]:

$$\left(\frac{d\alpha}{dt}\right)_{chem} = (k_1 + k_2\alpha^m)(1-\alpha)^n \qquad (7)$$

where k_1 and k_2 are temperature-dependent rate constants, and m and n represent empirical reaction parameters.

Obviously the alumina particles do not change the nature of the autocatalytic nth-order reaction kinetics: in the chemically controlled regime the $\frac{d\alpha}{dt}(\alpha)$ curves of all the investigated samples can be perfectly fitted to the Kamal model (equation (7)). The deviation of $\frac{d\alpha}{dt}$ from $(\frac{d\alpha}{dt})_{chem}$ results from mobility restrictions inside the network and marks the transition from the chemically to the diffusion-controlled regime of the respective reaction. The influence of the loss of

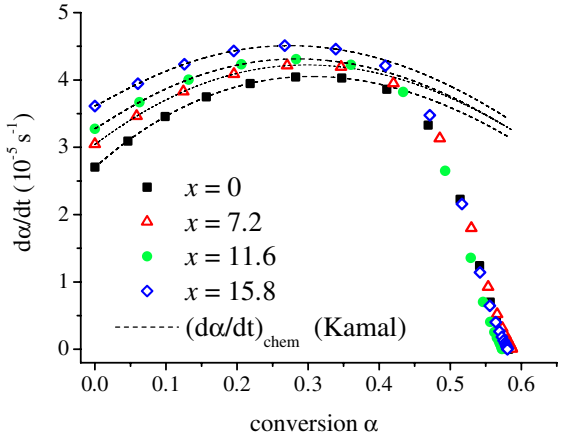

Figure 5. Isothermal cure of DER331–x% Al_2O_3–DETA nanocomposites at $T_{cure} = 298$ K: reaction rates $\frac{d\alpha}{dt}$ as a function of conversion α. The dashed lines represent the chemical conversions $(\frac{d\alpha}{dt})_{chem}$ and correspond to fits of the experimental data to the Kamal model.

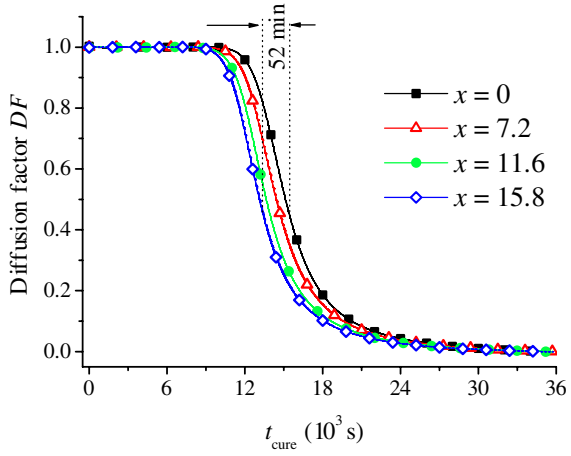

Figure 6. Isothermal cure of DER331–x% Al_2O_3–DETA nanocomposites at $T_{cure} = 298$ K: diffusion factor DF as a function of curing time t_{cure}.

molecular mobility on the reaction kinetics can be described by a diffusion factor [12] defined as

$$\mathrm{DF}(t) = \frac{\frac{d\alpha}{dt}}{\left(\frac{d\alpha}{dt}\right)_{chem}}. \qquad (8)$$

As long as the nanocomposites evolve in the chemically controlled regime DF = 1. Once the molecular mobility restrictions become significant the reactions progress in the diffusion-controlled regime and DF < 1 [12, 21]. Figure 6 shows how the diffusion factors of the investigated nanocomposites evolve as a function of curing time.

As can clearly be seen, the transition from the chemically to the diffusion-controlled regime occurs the earlier the higher the nanoparticle concentration. Thus, for instance, 52 min elapse between the respective transitions in the sample with 15.8% of Al_2O_3 and in the pure epoxy. During this time the reaction progresses in the pure system according

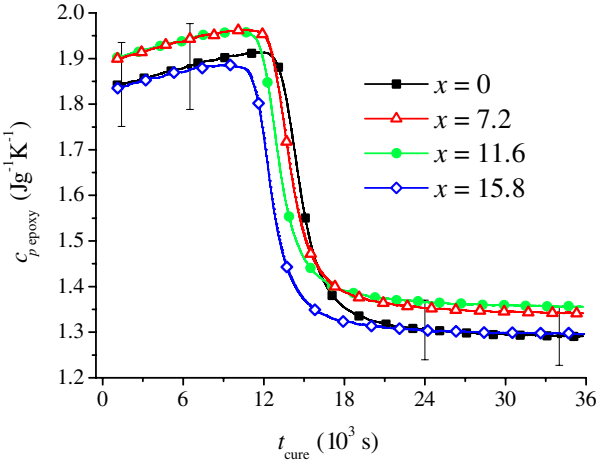

Figure 7. Isothermal cure of DER331–x% Al_2O_3–DETA nanocomposites at $T_{cure} = 298$ K: heat capacity per gram epoxy $c_{p\,epoxy}$ as a function of curing time t_{cure}.

to autocatalytic nth-order kinetics, whereas in the filled sample curing slows down. From this it follows that, in isothermal cure experiments, the loss of specific reaction heat in nanocomposites (table 1) mainly seems to be a consequence of molecular mobility restrictions whose importance increases with the nanoparticle content in the samples.

The loss of molecular mobility leads to chemical vitrification which can easily be visualized by a step decrease in the specific heat capacity. Figure 7 shows the modulus of the heat capacity per gram epoxy as a function of curing time for each nanocomposite.

As the specific heat capacity has been measured by means of TMDSC, it must be emphasized that the aforementioned step decrease always corresponds to a dynamic glass transition occurring when the experimental timescale crosses the intrinsic timescale of the respective evolving network structure. The epoxy part of the heat capacity has been evaluated using a simple mixing rule together with $c_{p\,Al_2O_3} = (0.91 \pm 0.05)$ J g^{-1} K^{-1}, the specific heat capacity of compacted Al_2O_3 nanopowder we have measured at $T_{cure} = 298$ K. Any deviation of the $c_{p\,epoxy}$ data from the results obtained for the pure system should thus be ascribed to the influence of the nanoparticles on the epoxy matrix.

Although the data do not systematically evolve when the nanoparticle concentration is changed, the $c_{p\,epoxy}$ values obtained for the different nanocomposites coincide within the margins of experimental accuracy in the liquid and in the glassy state of the samples. This leads us to adjust the curves to make them coincide at $t_{cure} = 0$. From a physical point of view we thus hypothesize that, at the very beginning of the isothermal cure experiments, the mixing rule we apply to determine the epoxy part of the specific heat capacity holds true perfectly.

From figure 8 it becomes clear that the Al_2O_3 nanoparticles strongly influence the chemical glass transition of the epoxy matrix. As a matter of fact both the vitrification time t_{vit} and the step height $\Delta c_{p\,epoxy}$ decrease with increasing filler concentration (figure 9(a)). We assume that the formation of interphases emerging between the polymer matrix and the

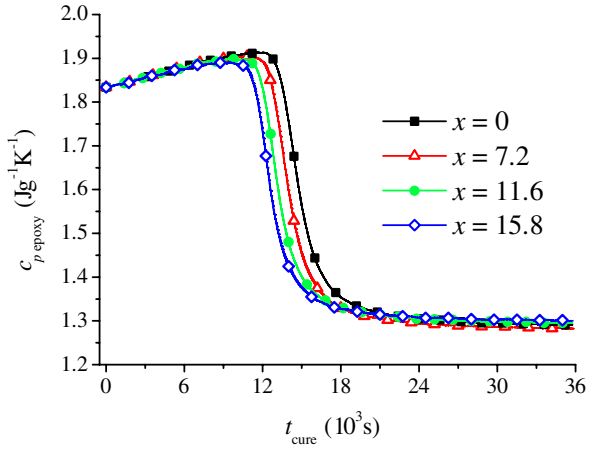

Figure 8. Isothermal cure of DER331–x% Al_2O_3–DETA nanocomposites at $T_{\mathrm{cure}} = 298$ K: heat capacity per gram epoxy $c_{p\ \mathrm{epoxy}}$ as a function of curing time t_{cure}. The curves correspond to those shown in figure 6 with the exception that they have been laid together at $t_{\mathrm{cure}} = 0$ s.

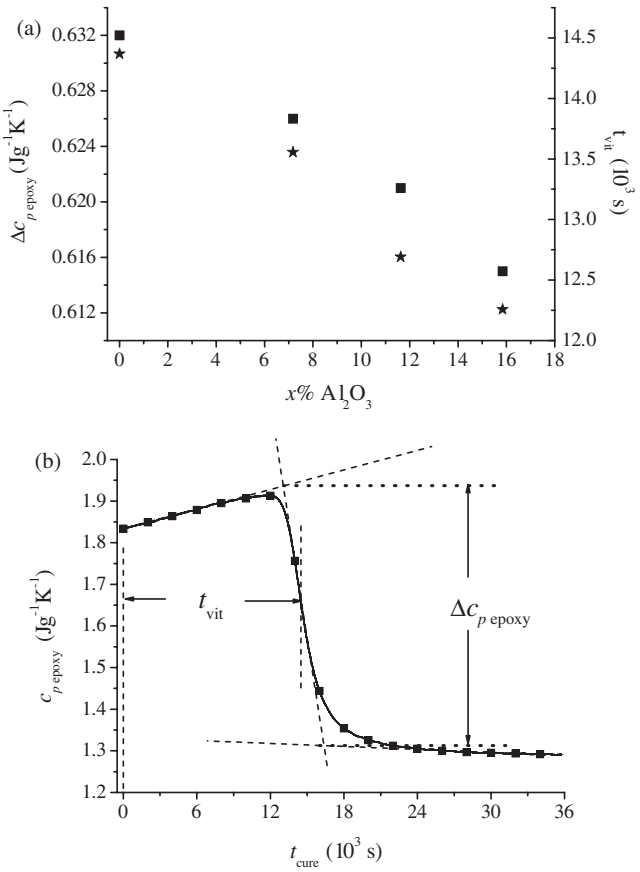

Figure 9. (a) Isothermal cure of DER331–x% Al_2O_3–DETA nanocomposites at $T_{\mathrm{cure}} = 298$ K: heat capacity step height $\Delta c_{p\ \mathrm{epoxy}}$ per gram epoxy (squares) and vitrification time t_{vit} (stars) as a function of Al_2O_3 mass concentration x. (b) Isothermal cure of DER331–0% Al_2O_3–DETA: illustration of the procedure leading to the determination of $\Delta c_{p\ \mathrm{epoxy}}$ and t_{vit}.

surfaces of the nanoparticles are responsible for the earlier occurrence of the vitrification in the presence of fillers. These domains with a structure different to the one of the epoxy bulk are due to interactions between the Al_2O_3 particles and the matrix. Several mechanisms can lead to the formation of interphases.

A first one concerns the catalytic action of the Al_2O_3 nanoparticles. The acceleration of the reaction at the beginning of cure of the filled systems indeed gives a strong hint to the presence of hydroxyl groups at the surface of the Al_2O_3 nanoparticles. Similar to the amine groups of the hardener, the hydroxyl groups can spend hydrogen atoms which are essential for the opening of oxirane rings of the resin or epoxy molecules [23]. The hydroxyl groups thus catalyse the curing reaction and contribute to increasing the cross-linking density in the vicinity of the nanoparticles. As already mentioned the contamination of the nanocomposites with water is little probable but cannot be excluded. H_2O molecules would also have a strong catalytic effect on the epoxy–amine reaction.

Other possible processes have been reported in the literature to play a role when metal-oxide surfaces are coated with adhesive epoxy mixtures.

(i) *Electromagnetic bonding*. Resin and epoxy molecules are known to have a high polarity due to the presence of aliphatic hydroxyl and ether groups. These polar groups serve as sites for the formation of strong electromagnetic bonding attractions (hydrogen bonds) between epoxy molecules and metal oxides [23].

(ii) *Mechanical bonding*. Mechanical bonding can be relevant if the surfaces of the metal oxides are porous or fibrous: resin and hardener molecules penetrate into the cavities as long as the adhesive mixture is in a liquid state. Upon curing the epoxy molecules become mechanically embedded into the porous structure [23].

(iii) *Organo-metallic complex formation*. In recently published works [24–26] it has been shown that resin—hardener mixtures applied onto native metal-oxide substrates lead to amine chemisorptions followed by a partial dissolution of the oxide layer. The amines combine with the metallic cations and form organo-metallic complexes (chelates) which diffuse into the resin–hardener mixture to form a network in competition with the epoxy.

While there is direct experimental evidence for the catalytic action of the nanoparticles it remains to be clarified how far the results established for the interaction of metal-oxide layers with the resin–hardener mixtures are applicable to the nanocomposites. Contrary to (i) and (ii) the formation of an additional network involving organo-metallic complexes (mechanism (iii)) would deplete the hardener content of the epoxy matrix. As a consequence the reaction heat per gram epoxy could be smaller in the nanocomposites than in the pure system. The nanocomposites would thus be expected to produce the same reaction heat per gram epoxy as the pure system, if their respective matrices contained an excess of hardener molecules. We, however, showed (to be published) that, in the filled systems, similar to the neat epoxy, the mass ratio of hardener and resin corresponding to a maximum of specific reaction heat corresponds to 14 g/100 g.

Looking at the $c_{p\ \mathrm{epoxy}}(t_{\mathrm{cure}})$ curves it becomes clear that the interphases only manifest themselves at the chemical glass

transition which competes with the structure formation and transforms the nanocomposites from a liquid–rubbery state into a glassy state. Neither in the liquid–rubbery phase nor in the glassy phase an influence of the nanoparticles on the evolution of the specific heat capacity can be resolved. In the liquid–rubbery phase ($t < t_{vit}$) the structure formation is well known to go with entropy production which leads to an increase of the specific heat capacity [27–29]. In the glassy state, the specific heat capacity is mainly determined by contributions of phonons to the internal energy. Obviously, if specific contributions of the filled systems to the phonon bath exist, they cannot be resolved with TMDSC. Interphases force the chemical vitrification to occur at earlier curing times. They are thus responsible for the reduction of molecular mobility.

In summary, the nanoparticles play a double role in the course of isothermal curing. On the one hand they accelerate the growth of the network, while, on the other hand, they have to be made responsible for a significant reduction of molecular mobility at a later stage of the network formation process. As a result of the latter, vitrification and hence the transition from the chemically controlled to the diffusion-controlled regime occur the earlier the higher the nanoparticle concentration. Finally, in the filled systems the gain of reaction heat at the beginning of the isothermal reactions is overcompensated by the loss of reaction heat resulting from the earlier transition to the diffusion-controlled regime. This argument allows for understanding the systematic reduction of reaction heat per gram epoxy when the nanoparticle concentration increases. Astonishingly the molecular mobility restrictions imparted by the nanoparticles cannot be completely removed by increasing the thermal agitation. As a matter of fact, in dynamically cured samples, the total reaction heat per gram epoxy continues to systematically decrease with increasing nanoparticle concentration. A still unknown mechanism has to be made responsible for the hindrance of molecular movements in the presence of nanoparticles.

It is well known from the literature that the zero-shear viscosity η_0 increases with the mass average molecular mass of the molecules in the course of polymer network formation. In order to study the influence of the nanoparticles on the network growth we measured the zero-shear viscosities of the nanocomposites upon curing at room temperature. Figure 10(a) shows how the zero-shear viscosities of the DER331–x% Al_2O_3–DETA (x = 0, 7.2, 11.6 and 15.8) systems change as a function of curing time. At the beginning of the reaction the zero-shear viscosities of the low molecular mixtures are small and systematically increase with the nanoparticle concentration x (figure 10(b)). Obviously the divergence of the zero-shear viscosity starts the earlier the higher the nanoparticle concentration x. We tend to claim that the divergence of the zero-shear viscosity is indicative for gelation in the samples we have investigated. In figure 10(c), $c_{p\ \mathrm{epoxy}}$ and η_0 are represented as a function of curing time t_{cure} for the DER331–15.8% mass Al_2O_3–DETA sample. An operative percolation time $t_{op\ gel}$ has been estimated by extrapolating $\eta_0^{-1}(t)$ to zero in the final stage of gelation [30]. Although the method lacks accuracy, the large difference $t_{vit} - t_{op\ gel} \approx 5400$ s gives a first

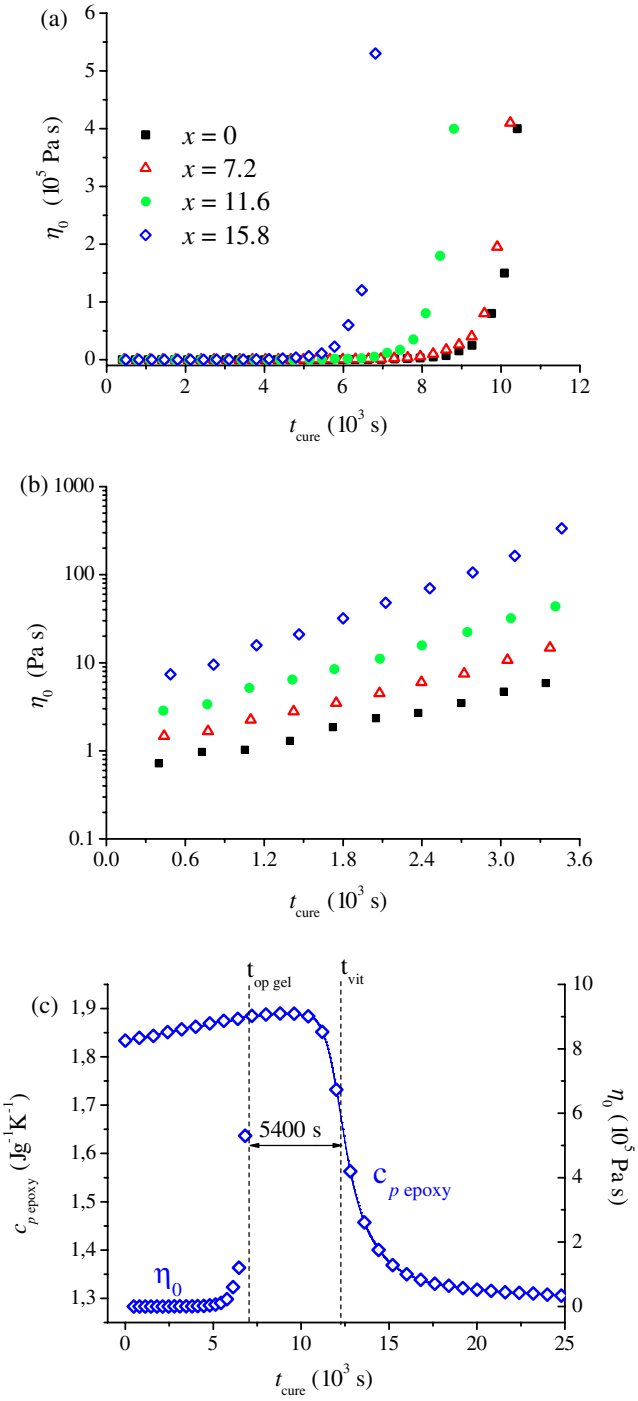

Figure 10. (a) Isothermal cure of DER331–x% mass Al_2O_3–DETA nanocomposites at T_{cure} = 298 K: zero-shear viscosity η_0 as a function of curing time t_{cure}. (b) Dependence of η_0 on the nanoparticle concentration at the beginning of the curing reaction. (c) $c_{p\ \mathrm{epoxy}}(t)$ and $\eta_0(t)$ as a function of curing time t_{cure} for DER331–15.8% mass Al_2O_3–DETA.

hint of gelation occurring before chemical vitrification in the considered sample. Moreover it has to be stressed that in our experiments t_{vit} corresponds to a dynamic glass transition and that static vitrification would even occur at a later stage of the reaction. As $t_{vit} - t_{op\ gel}$ increases from approximately 3700 s to about 5400 s when the nanoparticle concentration grows from

0 to 15.8 mass per cent we assume that (i) in all the samples gelation precedes vitrification and (ii) nanoparticles have an influence on percolation by contributing to the size and average molecular weight of the macromolecules. Further experiments are currently running to strengthen this argument.

4. Conclusion

The isothermal cure of an epoxy-based thermoset filled with Al_2O_3 nanoparticles was investigated by means of TMDSC and rheology. It was shown that the nature of the reaction kinetics is not changed by the nanoparticles: independently of the filler concentration the nanocomposites obey autocatalytic *n*th-order kinetics. In contrast the nanoparticles have an influence on the specific reaction heat produced upon isothermal cure and on chemical vitrification. With increasing nanoparticle concentration the specific reaction heat decreases. Obviously the gain of reaction heat due to a catalytic action of the Al_2O_3 particles is overcompensated by the loss of reaction heat resulting from an earlier transition from the liquid–rubbery state to the glassy state. In the filled systems the formation of interphases is made responsible for the occurrence of chemical vitrification at lower curing times. Rheologic measurements of the zero-shear viscosity give evidence for an accelerated growth of the network in the presence of nanoparticles and an earlier occurrence of gelation. The reduction of molecular mobility by the interphases is so important that even thermal activation by continuously increasing the temperature of the samples in the course of dynamic cure experiments does not suffice to achieve the same specific reaction heat as in the neat system.

References

[1] Wetzel B, Haupert F and Zhang M Q 2003 Epoxy nanocomposites with high mechanical and tribological performance *Compos. Sci. Technol.* **63** 2055–67

[2] Ji Q L, Zhang M Q, Rong M Z, Wetzel B and Friedrich K 2004 Tribological properties of surface modified nano-alumina/epoxy composites *J. Mater. Sci.* **39** 6487–93

[3] Han J T and Cho K 2006 Nanoparticle-induced enhancement in fracture toughness of highly loaded epoxy composites over a wide temperature range *J. Mater. Sci.* **41** 4239–45

[4] Kinloch A J and Taylor A C 2006 The mechanical properties and fracture behaviour of epoxy-inorganic micro- and nano-composites *J. Mater. Sci.* **41** 3271–97

[5] Kinloch A J, Masania K, Taylor A C, Sprenger S and Egan D 2008 The fracture of glass-fiber-reinforced epoxy composites using nanoparticle-modified matrices *J. Mater. Sci.* **43** 1151–54

[6] Dudkin B N, Zainullin G G, Krivoshapkin P V, Krivoshapkina E F and Ryazanov M A 2008 Influence of nanoparticles and nanofibers of aluminium oxide on the properties of epoxy composites *Glass Phys. Chem.* **34** 187–91

[7] Zhang H, Zhang Z, Friedrich K and Eger Ch 2006 Property improvements of *in situ* epoxy nanocomposites with reduced interparticle distance at high nanosilica content *Acta Mater.* **54** 1833–42

[8] Zhai L L, Ling G P and Wang Y W 2007 Effect of nano-Al_2O_3 on adhesion strength of epoxy adhesive and steel *Int. J. Adhes. Adhes.* **28** 23–8

[9] Gorbatkina Y A, Ivanova-Mumzhieva V G and Ul'yanova T M 2007 Adhesiveness of an epoxy oligomer filled with aluminum oxide powders *Polym. Sci.* C **49** 131–4

[10] Paz-Abuin S, Lopez-Quintela A, Pellin M P, Varela M and Prendes P 1997 Autoacceleration and inhibition: free volume. Epoxy-amine kinetics *J. Polym. Sci.* A **36** 1001–16

[11] Altmann N, Halley P J, Cooper-White J and Lange J 2001 The effect of silica fillers on the gelation and vitrification of highly filled epoxy–amine thermosets *Macromol. Symp.* **169** 171–7

[12] Van Assche G, Van Hemelrijck A, Rahier H and Van Mele B 1995 Modulated differential scanning calorimetry: isothermal cure and vitrification of thermosetting systems *Thermochim. Acta* **268** 121–42

[13] Swier S, Van Assche G, Van Hemelrijck A, Rahier H, Verdonck E and Van Mele B 1998 Characterization of reacting polymer systems by temperature-modulated differential scanning calorimetry *J. Therm. Anal.* **54** 585–604

[14] Pascault J P, Sautereau H, Verdu J and Williams R J J 2002 *Thermosetting Polymers* (New York: Dekker) chapter 3

[15] Gupta R K 2000 *Polymer and Composite Rheology* 2nd edn (New York: Dekker)

[16] Halley P J and Mackay M E 1996 Chemorheology of thermosets—an overview *Polym. Eng. Sci.* **36** 593–609

[17] Habenicht G 2006 *Kleben: Grundlagen, Technologien, Anwendungen* 5th edn (Berlin: Springer) p 77

[18] Ellis B 1993 Introduction to the chemistry, synthesis, manufacture and characterization of epoxy resins *Chemistry and Technology of Epoxy Resins* ed B Ellis (London: Blackie Academic & Professional)

[19] Schawe J E K 1995 A comparison of different evaluation methods in modulated temperature DSC *Thermochim. Acta* **260** 1–16

[20] Bockenheimer C, Fata D and Possart W 2004 New aspects of aging in epoxy networks. I. Thermal aging *J. Appl. Polym. Sci.* **91** 361–68

[21] Schawe J E K 2002 A description of chemical and diffusion control in isothermal kinetics of cure kinetics *Thermochim. Acta* **388** 299–312

[22] Kamal M R 1974 Thermoset characterization for moldability analysis *Polym. Eng. Sci.* **14** 231–9

[23] Schmidt R G and Bell J P 1986 Epoxy adhesion to metals *Epoxy resins and composites II* ed K Dusek (Berlin: Springer)

[24] Mercier D, Rouchaud J C and Barthès-Labrousse M G 2008 Interaction of amines with native aluminium oxide layers in non-aqueous environment: application to the understanding of the formation of epoxy–amine/metal interphases *Appl. Surf. Sci.* **254** 6495–503

[25] Aufray M and Roche A A 2007 Epoxy-amine/metal interphases: influences from sharp needle-like crystal formation *Int. J. Adhes. Adhes.* **27** 387–93

[26] Aufray M and Roche A A 2008 Is gold always chemically passive? Study and comparison of the epoxy–amine/metals interphases *Appl. Surf. Sci.* **254** 1936–41

[27] Schawe J E K and Alig I 2001 Heat capacity relaxation during polymer network formation: limitations of equilibria descriptions *Colloid Polym. Sci.* **279** 1169–76

[28] Ferrari C, Salvetti G, Tombari E and Johari G P 1996 Specific heat relaxation during macromolecule growth *Phys. Rev.* E **54** 1058–61

[29] Viciosa M T, Hoyo J Q, Dionisio M and Ribelles J L G 2007 Temperature modulated DSC study of the kinetics of free radical isothermal network polymerization *J. Therm. Anal. Calorim.* **90** 407–14

[30] Malkin A Ya and Kulichikhin S G 1991 Rheokinetics of curing *Adv. Polym. Sci.* **101** 217–57